Search for New Heavy Particles decaying to $Z^0Z^0 \to eeee$ in $p\bar{p}$ Collisions at $\sqrt{s} = \mathbf{1.96}$ TeV

T. Aaltonen,[23] J. Adelman,[13] T. Akimoto,[54] M.G. Albrow,[17] B. Álvarez González,[11] S. Amerio,[42] D. Amidei,[34] A. Anastassov,[51] A. Annovi,[19] J. Antos,[14] M. Aoki,[24] G. Apollinari,[17] A. Apresyan,[47] T. Arisawa,[56] A. Artikov,[15] W. Ashmanskas,[17] A. Attal,[3] A. Aurisano,[52] F. Azfar,[41] P. Azzi-Bacchetta,[42] P. Azzurri,[45] N. Bacchetta,[42] W. Badgett,[17] A. Barbaro-Galtieri,[28] V.E. Barnes,[47] B.A. Barnett,[25] S. Baroiant,[7] V. Bartsch,[30] G. Bauer,[32] P.-H. Beauchemin,[33] F. Bedeschi,[45] P. Bednar,[14] S. Behari,[25] G. Bellettini,[45] J. Bellinger,[58] A. Belloni,[22] D. Benjamin,[16] A. Beretvas,[17] J. Beringer,[28] T. Berry,[29] A. Bhatti,[49] M. Binkley,[17] D. Bisello,[42] I. Bizjak,[30] R.E. Blair,[2] C. Blocker,[6] B. Blumenfeld,[25] A. Bocci,[16] A. Bodek,[48] V. Boisvert,[48] G. Bolla,[47] A. Bolshov,[32] D. Bortoletto,[47] J. Boudreau,[46] A. Boveia,[10] B. Brau,[10] A. Bridgeman,[24] L. Brigliadori,[5] C. Bromberg,[35] E. Brubaker,[13] J. Budagov,[15] H.S. Budd,[48] S. Budd,[24] K. Burkett,[17] G. Busetto,[42] P. Bussey,[21] A. Buzatu,[33] K. L. Byrum,[2] S. Cabrera[r],[16] M. Campanelli,[35] M. Campbell,[34] F. Canelli,[17] A. Canepa,[44] D. Carlsmith,[58] R. Carosi,[45] S. Carrillo[l],[18] S. Carron,[33] B. Casal,[11] M. Casarsa,[17] A. Castro,[5] P. Catastini,[45] D. Cauz,[53] M. Cavalli-Sforza,[3] A. Cerri,[28] L. Cerrito[p],[30] S.H. Chang,[27] Y.C. Chen,[1] M. Chertok,[7] G. Chiarelli,[45] G. Chlachidze,[17] F. Chlebana,[17] K. Cho,[27] D. Chokheli,[15] J.P. Chou,[22] G. Choudalakis,[32] S.H. Chuang,[51] K. Chung,[12] W.H. Chung,[58] Y.S. Chung,[48] C.I. Ciobanu,[24] M.A. Ciocci,[45] A. Clark,[20] D. Clark,[6] G. Compostella,[42] M.E. Convery,[17] J. Conway,[7] B. Cooper,[30] K. Copic,[34] M. Cordelli,[19] G. Cortiana,[42] F. Crescioli,[45] C. Cuenca Almenar[r],[7] J. Cuevas[o],[11] R. Culbertson,[17] J.C. Cully,[34] D. Dagenhart,[17] M. Datta,[17] T. Davies,[21] P. de Barbaro,[48] S. De Cecco,[50] A. Deisher,[28] G. De Lentdecker[d],[48] G. De Lorenzo,[3] M. Dell'Orso,[45] L. Demortier,[49] J. Deng,[16] M. Deninno,[5] D. De Pedis,[50] P.F. Derwent,[17] G.P. Di Giovanni,[43] C. Dionisi,[50] B. Di Ruzza,[53] J.R. Dittmann,[4] M. D'Onofrio,[3] S. Donati,[45] P. Dong,[8] J. Donini,[42] T. Dorigo,[42] S. Dube,[51] J. Efron,[38] R. Erbacher,[7] D. Errede,[24] S. Errede,[24] R. Eusebi,[17] H.C. Fang,[28] S. Farrington,[29] W.T. Fedorko,[13] R.G. Feild,[59] M. Feindt,[26] J.P. Fernandez,[31] C. Ferrazza,[45] R. Field,[18] G. Flanagan,[47] R. Forrest,[7] S. Forrester,[7] M. Franklin,[22] J.C. Freeman,[28] I. Furic,[18] M. Gallinaro,[49] J. Galyardt,[12] F. Garberson,[10] J.E. Garcia,[45] A.F. Garfinkel,[47] K. Genser,[17] H. Gerberich,[24] D. Gerdes,[34] S. Giagu,[50] V. Giakoumopolou[a],[45] P. Giannetti,[45] K. Gibson,[46] J.L. Gimmell,[48] C.M. Ginsburg,[17] N. Giokaris[a],[15] M. Giordani,[53] P. Giromini,[19] M. Giunta,[45] V. Glagolev,[15] D. Glenzinski,[17] M. Gold,[36] N. Goldschmidt,[18] A. Golossanov,[17] G. Gomez,[11] G. Gomez-Ceballos,[32] M. Goncharov,[52] O. González,[31] I. Gorelov,[36] A.T. Goshaw,[16] K. Goulianos,[49] A. Gresele,[42] S. Grinstein,[22] C. Grosso-Pilcher,[13] R.C. Group,[17] U. Grundler,[24] J. Guimaraes da Costa,[22] Z. Gunay-Unalan,[35] C. Haber,[28] K. Hahn,[32] S.R. Hahn,[17] E. Halkiadakis,[51] A. Hamilton,[20] B.-Y. Han,[48] J.Y. Han,[48] R. Handler,[58] F. Happacher,[19] K. Hara,[54] D. Hare,[51] M. Hare,[55] S. Harper,[41] R.F. Harr,[57] R.M. Harris,[17] M. Hartz,[46] K. Hatakeyama,[49] J. Hauser,[8] C. Hays,[41] M. Heck,[26] A. Heijboer,[44] B. Heinemann,[28] J. Heinrich,[44] C. Henderson,[32] M. Herndon,[58] J. Heuser,[26] S. Hewamanage,[4] D. Hidas,[16] C.S. Hill[c],[10] D. Hirschbuehl,[26] A. Hocker,[17] S. Hou,[1] M. Houlden,[29] S.-C. Hsu,[9] B.T. Huffman,[41] R.E. Hughes,[38] U. Husemann,[59] J. Huston,[35] J. Incandela,[10] G. Introzzi,[45] M. Iori,[50] A. Ivanov,[7] B. Iyutin,[32] E. James,[17] B. Jayatilaka,[16] D. Jeans,[50] E.J. Jeon,[27] S. Jindariani,[18] W. Johnson,[7] M. Jones,[47] K.K. Joo,[27] S.Y. Jun,[12] J.E. Jung,[27] T.R. Junk,[24] T. Kamon,[52] D. Kar,[18] P.E. Karchin,[57] Y. Kato,[40] R. Kephart,[17] U. Kerzel,[26] V. Khotilovich,[52] B. Kilminster,[38] D.H. Kim,[27] H.S. Kim,[27] J.E. Kim,[27] M.J. Kim,[17] S.B. Kim,[27] S.H. Kim,[54] Y.K. Kim,[13] N. Kimura,[54] L. Kirsch,[6] S. Klimenko,[18] M. Klute,[32] B. Knuteson,[32] B.R. Ko,[16] S.A. Koay,[10] K. Kondo,[56] D.J. Kong,[27] J. Konigsberg,[18] A. Korytov,[18] A.V. Kotwal,[16] J. Kraus,[24] M. Kreps,[26] J. Kroll,[44] N. Krumnack,[4] M. Kruse,[16] V. Krutelyov,[10] T. Kubo,[54] S. E. Kuhlmann,[2] T. Kuhr,[26] N.P. Kulkarni,[57] Y. Kusakabe,[56] S. Kwang,[13] A.T. Laasanen,[47] S. Lai,[33] S. Lami,[45] S. Lammel,[17] M. Lancaster,[30] R.L. Lander,[7] K. Lannon,[38] A. Lath,[51] G. Latino,[45] I. Lazzizzera,[42] T. LeCompte,[2] J. Lee,[48] J. Lee,[27] Y.J. Lee,[27] S.W. Lee[q],[52] R. Lefèvre,[20] N. Leonardo,[32] S. Leone,[45] S. Levy,[13] J.D. Lewis,[17] C. Lin,[59] C.S. Lin,[28] J. Linacre,[41] M. Lindgren,[17] E. Lipeles,[9] A. Lister,[7] D.O. Litvintsev,[17] T. Liu,[17] N.S. Lockyer,[44] A. Loginov,[59] M. Loreti,[42] L. Lovas,[14] R.-S. Lu,[1] D. Lucchesi,[42] J. Lueck,[26] C. Luci,[50] P. Lujan,[28] P. Lukens,[17] G. Lungu,[18] L. Lyons,[41] J. Lys,[28] R. Lysak,[14] E. Lytken,[47] P. Mack,[26] D. MacQueen,[33] R. Madrak,[17] K. Maeshima,[17] K. Makhoul,[32] T. Maki,[23] P. Maksimovic,[25] S. Malde,[41] S. Malik,[30] G. Manca,[29] A. Manousakis[a],[15] F. Margaroli,[47] C. Marino,[26] C.P. Marino,[24] A. Martin,[59] M. Martin,[25] V. Martin[j],[21] M. Martínez,[3] R. Martínez-Ballarín,[31] T. Maruyama,[54] P. Mastrandrea,[50] T. Masubuchi,[54] M.E. Mattson,[57] P. Mazzanti,[5] K.S. McFarland,[48] P. McIntyre,[52] R. McNulty[i],[29] A. Mehta,[29] P. Mehtala,[23] S. Menzemer[k],[11] A. Menzione,[45] P. Merkel,[47] C. Mesropian,[49] A. Messina,[35] T. Miao,[17] N. Miladinovic,[6] J. Miles,[32] R. Miller,[35] C. Mills,[22] M. Milnik,[26] A. Mitra,[1] G. Mitselmakher,[18] H. Miyake,[54] S. Moed,[22] N. Moggi,[5] C.S. Moon,[27] R. Moore,[17] M. Morello,[45] P. Movilla Fernandez,[28] J. Mülmenstädt,[28] A. Mukherjee,[17] Th. Muller,[26] R. Mumford,[25] P. Murat,[17] M. Mussini,[5] J. Nachtman,[17] Y. Nagai,[54] A. Nagano,[54] J. Naganoma,[56] K. Nakamura,[54] I. Nakano,[39] A. Napier,[55] V. Necula,[16] C. Neu,[44] M.S. Neubauer,[24] J. Nielsen[f],[28] L. Nodulman,[2] M. Norman,[9] O. Norniella,[24] E. Nurse,[30] S.H. Oh,[16] Y.D. Oh,[27] I. Oksuzian,[18] T. Okusawa,[40] R. Oldeman,[29] R. Orava,[23] K. Osterberg,[23] S. Pagan Griso,[42] C. Pagliarone,[45] E. Palencia,[17] V. Papadimitriou,[17] A. Papaikonomou,[26] A.A. Paramonov,[13] B. Parks,[38] S. Pashapour,[33] J. Patrick,[17] G. Pauletta,[53] M. Paulini,[12] C. Paus,[32] D.E. Pellett,[7] A. Penzo,[53] T.J. Phillips,[16] G. Piacentino,[45] J. Piedra,[43] L. Pinera,[18] K. Pitts,[24] C. Plager,[8] L. Pondrom,[58] X. Portell,[3] O. Poukhov,[15] N. Pounder,[41] F. Prakoshyn,[15] A. Pronko,[17] J. Proudfoot,[2] F. Ptohos[h],[17] G. Punzi,[45] J. Pursley,[58] J. Rademacker[c],[41] A. Rahaman,[46] V. Ramakrishnan,[58] N. Ranjan,[47] I. Redondo,[31] B. Reisert,[17] V. Rekovic,[36] P. Renton,[41] M. Rescigno,[50] S. Richter,[26] F. Rimondi,[5] L. Ristori,[45] A. Robson,[21] T. Rodrigo,[11] E. Rogers,[24] S. Rolli,[55] R. Roser,[17] M. Rossi,[53] R. Rossin,[10] P. Roy,[33] A. Ruiz,[11] J. Russ,[12] V. Rusu,[17] H. Saarikko,[23] A. Safonov,[52] W.K. Sakumoto,[48] G. Salamanna,[50] O. Saltó,[3] L. Santi,[53] S. Sarkar,[50] L. Sartori,[45] K. Sato,[17] A. Savoy-Navarro,[43] T. Scheidle,[26] P. Schlabach,[17] E.E. Schmidt,[17] M.A. Schmidt,[13] M.P. Schmidt,[59] M. Schmitt,[37] T. Schwarz,[7] L. Scodellaro,[11] A.L. Scott,[10] A. Scribano,[45] F. Scuri,[45] A. Sedov,[47] S. Seidel,[36] Y. Seiya,[40] A. Semenov,[15] L. Sexton-Kennedy,[17] A. Sfyrla,[20] S.Z. Shalhout,[57] M.D. Shapiro,[28] T. Shears,[29] P.F. Shepard,[46] D. Sherman,[22] M. Shimojima[n],[54] M. Shochet,[13] Y. Shon,[58] I. Shreyber,[20] A. Sidoti,[45] P. Sinervo,[33] A. Sisakyan,[15] A.J. Slaughter,[17] J. Slaunwhite,[38] K. Sliwa,[55] J.R. Smith,[7] F.D. Snider,[17] R. Snihur,[33] M. Soderberg,[34] A. Soha,[7] S. Somalwar,[51] V. Sorin,[35] J. Spalding,[17] F. Spinella,[45] T. Spreitzer,[33] P. Squillacioti,[45] M. Stanitzki,[59] R. St. Denis,[21] B. Stelzer,[8] O. Stelzer-Chilton,[41] D. Stentz,[37] J. Strologas,[36] D. Stuart,[10] J.S. Suh,[27] A. Sukhanov,[18] H. Sun,[55] I. Suslov,[15] T. Suzuki,[54] A. Taffard[e],[24] R. Takashima,[39] Y. Takeuchi,[54] R. Tanaka,[39] M. Tecchio,[34] P.K. Teng,[1] K. Terashi,[49] J. Thom[g],[17] A.S. Thompson,[21] G.A. Thompson,[24] E. Thomson,[44] P. Tipton,[59] V. Tiwari,[12] S. Tkaczyk,[17] D. Toback,[52] S. Tokar,[14] K. Tollefson,[35] T. Tomura,[54] D. Tonelli,[17] S. Torre,[19] D. Torretta,[17] S. Tourneur,[43] W. Trischuk,[33] Y. Tu,[44] N. Turini,[45] F. Ukegawa,[54] S. Uozumi,[54] S. Vallecorsa,[20] N. van Remortel,[23] A. Varganov,[34] E. Vataga,[36] F. Vázquez[l],[18] G. Velev,[17] C. Vellidis[a],[45] V. Veszpremi,[47] M. Vidal,[31] R. Vidal,[17] I. Vila,[11] R. Vilar,[11] T. Vine,[30] M. Vogel,[36] I. Volobouev[q],[28] G. Volpi,[45] F. Würthwein,[9] P. Wagner,[44] R.G. Wagner,[2] R.L. Wagner,[17] J. Wagner-Kuhr,[26] W. Wagner,[26] T. Wakisaka,[40] R. Wallny,[8] S.M. Wang,[1] A. Warburton,[33] D. Waters,[30] M. Weinberger,[52] W.C. Wester III,[17] B. Whitehouse,[55] D. Whiteson[e],[44] A.B. Wicklund,[2] E. Wicklund,[17] G. Williams,[33] H.H. Williams,[44] P. Wilson,[17] B.L. Winer,[38] P. Wittich[g],[17] S. Wolbers,[17] C. Wolfe,[13] T. Wright,[34] X. Wu,[20] S.M. Wynne,[29]

A. Yagil,[9] K. Yamamoto,[40] J. Yamaoka,[51] T. Yamashita,[39] C. Yang,[59] U.K. Yang[m],[13] Y.C. Yang,[27] W.M. Yao,[28] G.P. Yeh,[17] J. Yoh,[17] K. Yorita,[13] T. Yoshida,[40] G.B. Yu,[48] I. Yu,[27] S.S. Yu,[17] J.C. Yun,[17] L. Zanello,[50] A. Zanetti,[53] I. Zaw,[22] X. Zhang,[24] Y. Zheng[b],[8] and S. Zucchelli[5]

(CDF Collaboration[*])

[1]*Institute of Physics, Academia Sinica, Taipei, Taiwan 11529, Republic of China*
[2]*Argonne National Laboratory, Argonne, Illinois 60439*
[3]*Institut de Fisica d'Altes Energies, Universitat Autonoma de Barcelona, E-08193, Bellaterra (Barcelona), Spain*
[4]*Baylor University, Waco, Texas 76798*
[5]*Istituto Nazionale di Fisica Nucleare, University of Bologna, I-40127 Bologna, Italy*
[6]*Brandeis University, Waltham, Massachusetts 02254*
[7]*University of California, Davis, Davis, California 95616*
[8]*University of California, Los Angeles, Los Angeles, California 90024*
[9]*University of California, San Diego, La Jolla, California 92093*
[10]*University of California, Santa Barbara, Santa Barbara, California 93106*
[11]*Instituto de Fisica de Cantabria, CSIC-University of Cantabria, 39005 Santander, Spain*
[12]*Carnegie Mellon University, Pittsburgh, PA 15213*
[13]*Enrico Fermi Institute, University of Chicago, Chicago, Illinois 60637*
[14]*Comenius University, 842 48 Bratislava, Slovakia; Institute of Experimental Physics, 040 01 Kosice, Slovakia*
[15]*Joint Institute for Nuclear Research, RU-141980 Dubna, Russia*
[16]*Duke University, Durham, North Carolina 27708*
[17]*Fermi National Accelerator Laboratory, Batavia, Illinois 60510*
[18]*University of Florida, Gainesville, Florida 32611*
[19]*Laboratori Nazionali di Frascati, Istituto Nazionale di Fisica Nucleare, I-00044 Frascati, Italy*
[20]*University of Geneva, CH-1211 Geneva 4, Switzerland*
[21]*Glasgow University, Glasgow G12 8QQ, United Kingdom*
[22]*Harvard University, Cambridge, Massachusetts 02138*
[23]*Division of High Energy Physics, Department of Physics, University of Helsinki and Helsinki Institute of Physics, FIN-00014, Helsinki, Finland*
[24]*University of Illinois, Urbana, Illinois 61801*
[25]*The Johns Hopkins University, Baltimore, Maryland 21218*
[26]*Institut für Experimentelle Kernphysik, Universität Karlsruhe, 76128 Karlsruhe, Germany*
[27]*Center for High Energy Physics: Kyungpook National University, Daegu 702-701, Korea; Seoul National University, Seoul 151-742, Korea; Sungkyunkwan University, Suwon 440-746, Korea; Korea Institute of Science and Technology Information, Daejeon, 305-806, Korea; Chonnam National University, Gwangju, 500-757, Korea*
[28]*Ernest Orlando Lawrence Berkeley National Laboratory, Berkeley, California 94720*
[29]*University of Liverpool, Liverpool L69 7ZE, United Kingdom*
[30]*University College London, London WC1E 6BT, United Kingdom*
[31]*Centro de Investigaciones Energeticas Medioambientales y Tecnologicas, E-28040 Madrid, Spain*
[32]*Massachusetts Institute of Technology, Cambridge, Massachusetts 02139*
[33]*Institute of Particle Physics: McGill University, Montréal, Canada H3A 2T8; and University of Toronto, Toronto, Canada M5S 1A7*
[34]*University of Michigan, Ann Arbor, Michigan 48109*
[35]*Michigan State University, East Lansing, Michigan 48824*
[36]*University of New Mexico, Albuquerque, New Mexico 87131*
[37]*Northwestern University, Evanston, Illinois 60208*
[38]*The Ohio State University, Columbus, Ohio 43210*
[39]*Okayama University, Okayama 700-8530, Japan*
[40]*Osaka City University, Osaka 588, Japan*
[41]*University of Oxford, Oxford OX1 3RH, United Kingdom*
[42]*University of Padova, Istituto Nazionale di Fisica Nucleare, Sezione di Padova-Trento, I-35131 Padova, Italy*
[43]*LPNHE, Universite Pierre et Marie Curie/IN2P3-CNRS, UMR7585, Paris, F-75252 France*
[44]*University of Pennsylvania, Philadelphia, Pennsylvania 19104*

[45]Istituto Nazionale di Fisica Nucleare Pisa, Universities of Pisa, Siena and Scuola Normale Superiore, I-56127 Pisa, Italy
[46]University of Pittsburgh, Pittsburgh, Pennsylvania 15260
[47]Purdue University, West Lafayette, Indiana 47907
[48]University of Rochester, Rochester, New York 14627
[49]The Rockefeller University, New York, New York 10021
[50]Istituto Nazionale di Fisica Nucleare, Sezione di Roma 1, University of Rome "La Sapienza," I-00185 Roma, Italy
[51]Rutgers University, Piscataway, New Jersey 08855
[52]Texas A&M University, College Station, Texas 77843
[53]Istituto Nazionale di Fisica Nucleare, University of Trieste/ Udine, Italy
[54]University of Tsukuba, Tsukuba, Ibaraki 305, Japan
[55]Tufts University, Medford, Massachusetts 02155
[56]Waseda University, Tokyo 169, Japan
[57]Wayne State University, Detroit, Michigan 48201
[58]University of Wisconsin, Madison, Wisconsin 53706
[59]Yale University, New Haven, Connecticut 06520

We report the results of a search for the anomalous production of a massive particle decaying to four electrons via two Z^0 bosons in 1.1 fb^{-1} of $p\bar{p}$ collisions at $\sqrt{s}$ =1.96 TeV collected by the CDF II detector at Fermilab. We employ optimized electron identification criteria to maximize acceptance and efficiency. We estimate the backgrounds in the invariant mass range 500 - 1000 GeV/c^2 to be 0.028 ± 0.009 (stat) $\pm$ 0.011 (syst) events. We observe zero events in this search region. Assuming a Randall-Sundrum graviton production model, we set 95% CL limits on $\sigma \times \mathrm{BF}(G \rightarrow Z^0 Z^0) < 4 - 6$ pb, depending on the graviton mass.

PACS numbers:

I. INTRODUCTION

We present a search for new heavy particles "G" in the decay mode $G \rightarrow Z^0 Z^0 \rightarrow eeee$ in $\bar{p}p$ collisions at $\sqrt{s} = 1.96$ TeV performed with the CDF II detector at the Fermilab Tevatron. Previous analyses of double gauge boson production at the Tevatron have focused on standard model production [1–4]. Here, we present for the first time a search for massive particles G which decay to $Z^0 Z^0$ which could indicate physics beyond the standard model.

The goal of this search is to be sensitive to production of any massive particle which could decay to $Z^0 Z^0$, that is, to avoid focusing on any one specific model; however, for the purpose of quantifying acceptance for this search, we consider the virtual production of gravitons in a simple Randall-Sundrum (RS1) scenario [5, 6]. In this model, the geometry consists of two 3-branes which confine the standard model sector separated from each other by a single extra dimension. One can look for evidence of the extra dimension at particle colliders in the form of a Kaluza-Klein tower of discrete, massive gravitons. In the RS1 scenario, the gravitons predominantly decay to jets, and the remaining modes are W^+W^- ($\sim 10\%$), $Z^0 Z^0$ ($\sim 5\%$), $\gamma\gamma$ ($\sim 5\%$), and ll ($\sim 2\%$ per lepton)[7]. Searches for the decays of such particles to photons and electrons have been performed [8–10]. If the couplings to leptons and photons are suppressed relative to the couplings to gauge bosons [11], such a particle might escape detection in these searches. Here, we have searched for massive particles in their decays to Z^0 bosons.

In the leptonic final states of Z^0 decay, the

*With visitors from [a]University of Athens, 15784 Athens, Greece, [b]Chinese Academy of Sciences, Beijing 100864, China, [c]University of Bristol, Bristol BS8 1TL, United Kingdom, [d]University Libre de Bruxelles, B-1050 Brussels, Belgium, [e]University of California Irvine, Irvine, CA 92697, [f]University of California Santa Cruz, Santa Cruz, CA 95064, [g]Cornell University, Ithaca, NY 14853, [h]University of Cyprus, Nicosia CY-1678, Cyprus, [i]University College Dublin, Dublin 4, Ireland, [j]University of Edinburgh, Edinburgh EH9 3JZ, United Kingdom, [k]University of Heidelberg, D-69120 Heidelberg, Germany, [l]Universidad Iberoamericana, Mexico D.F., Mexico, [m]University of Manchester, Manchester M13 9PL, England, [n]Nagasaki Institute of Applied Science, Nagasaki, Japan, [o]University de Oviedo, E-33007 Oviedo, Spain, [p]Queen Mary, University of London, London, E1 4NS, England, [q]Texas Tech University, Lubbock, TX 79409, [r]IFIC(CSIC-Universitat de Valencia), 46071 Valencia, Spain,

expected signal from the model described above is small, as are the backgrounds. In order to maximize acceptance and efficiency for the four-electron signature, we use optimized calorimetric electron identification criteria, select electron candidates identified as isolated tracks where there is no calorimeter coverage, and use low electron energy thresholds.

The organization of this article is as follows: first, we describe the components of the CDF II detector relevant to this search and summarize the data sample and event selection criteria. Then we describe the background estimation, report the results of the search, and interpret the results in the context of the lightest massive RS1 graviton.

II. THE CDF II DETECTOR

This analysis uses 1.1 fb^{-1} of $p\bar{p}$ collisions collected by the CDF II detector, a general purpose magnetic spectrometer. We briefly describe the components of the detector relevant to this search here. A complete description can be found elsewhere [12].

A combination of tracking systems reconstruct the trajectories and measure momenta of charged particles in a 1.4T solenoidal magnetic field. Trajectories of charged particles are reconstructed using an eight-layer silicon microstrip vertex tracker [13] at radii $1.3 < r < 29$ cm [14], and a 96-layer open-cell drift chamber (COT) providing eight superlayers of alternating axial and stereo position measurements [15]. The COT allows track reconstruction at large radii $43 < r < 132$ cm in the region $|\eta| < 1.6$, and provides full geometric coverage for $|\eta| < 1.0$.

Outside the tracking volume, segmented electromagnetic (EM) lead-scintillator and hadronic (HAD) iron-scintillator sampling calorimeters measure particle energies [16]. In the central region ($|\eta| < 1.1$), the calorimeters are arranged in a projective-tower cylindrical geometry, divided azimuthally into 15° wedges which measure EM energies with a resolution of $[\sigma(E)/E]^2 = (13.5\%)^2/E_T + (2\%)^2$. In the region covered by the forward calorimeter ($1.1 < |\eta| < 3.6$), the calorimeters are arranged in an azimuthally-symmetric disk geometry and measure EM energies with a resolution of $[\sigma(E)/E]^2 = (16.0\%)^2/E + (1\%)^2$. Wire chambers (scintillator strips) embedded in the central (forward) EM calorimeters at the electromagnetic shower maximum ($\sim 6X_0$) provide position and lateral shower development measurements used to identify electrons by their characteristic energy-deposition distribution. The beam luminosity is determined by measuring the inelastic $p\bar{p}$ collision rate with gas Cherenkov detectors[17], located in the region $3.7 < |\eta| < 4.7$.

III. EVENT SELECTION

Events are selected for collection by a three-level trigger system. We search in data collected by triggering on a central high-momentum electron. Each of two trigger paths used requires an energy cluster in the central calorimeter and a track which projects to the energy cluster. The primary trigger path requires a clustered transverse energy $E_{\rm T} > 18$ GeV, transverse momentum of the associated track $p_T > 9$ GeV/c, the ratio of energy measured in the hadronic to electromagnetic calorimeters, $E_{HAD}/E_{EM} < 0.125$ and a lateral shower profile consistent with an electron. The second trigger path requires a cluster with $E_{\rm T} > 70$ GeV and an associated track with $p_T > 15$ GeV/c.

We select events containing one "seed" electron which satisfies trigger requirements and those listed in Table I, and three other electrons which satisfy either the central, forward, or track requirements in Table I. To maximize acceptance and efficiency for events containing four electrons, we select three other electron candidates using optimized identification and kinematic criteria in the central or forward calorimeters, and from isolated tracks pointing to uninstrumented regions of the calorimeters.

Electron candidates are formed in the central and forward calorimeters from isolated energy deposits with $E_{\rm T} \geq 5$ GeV. An electron is considered to be isolated in the calorimeter if the sum of the transverse energy detected within a cone $\Delta R \equiv \sqrt{(\Delta\eta)^2 + (\Delta\phi)^2} \leq 0.4$, minus the electron $E_{\rm T}$, is less than 20% of the electron $E_{\rm T}$. For clusters in the central calorimeter, where tracking efficiency is optimal, we require that a track reconstructed in the COT project to the cluster. Tracks must include measurements in at least three axial and two stereo superlayers of the COT, and the track coordinate along the beam direction, z_0, must also lie within the nominal extent of the interaction region, $|z_0| < 60$ cm. To reduce backgrounds from hadrons misidentified as electrons, central candidates must also satisfy an energy-dependent requirement $E_{HAD}/E_{EM} < 0.055 + 0.00045\,\mathrm{GeV}^{-1} \times E_{EM}$. Forward candidates must have $E_{HAD}/E_{EM} < 0.05$ and lie within $1.1 < |\eta| < 2.5$.

The "seed" electron candidate must satisfy the above requirements to be reconstructed in the central calorimeter, and satisfy additional selection criteria imposed by the trigger. Specifically, the "seed" electron must also have $E_{\mathrm{T}} \geq 20$ GeV, satisfy the same lateral shower profile requirement as the triggering one, and have an associated track with $p_T \geq 10$ GeV/c.

Some calorimeter acceptance for electrons is lost in 24 one-degree gaps in ϕ between the central calorimeter projective wedges, a region at $0.7 < \eta < 1.0$ and $75^\circ < \phi < 90^\circ$ which accommodates cables and cryogenic utilities for the solenoid, a gap between central calorimeter arches at $\eta = 0$, and the gap at the junction between the central and forward calorimeters at $1.0 < |\eta| < 1.2$. Together, these regions add up to approximately 17% of the solid angle for $|\eta| < 1.2$, which for a four-lepton final state represents an acceptance loss of approximately half.

We recover acceptance by forming electron candidates from isolated tracks which project to the gaps between instrumented regions of the calorimeter. A track is defined to be isolated in the tracking chamber if the transverse momentum of the track is more than 90% of the total transverse momentum of all tracks within a cone $\Delta R \leq 0.4$ around the candidate track. We require track electron candidates be consistent with originating from prompt decays by requiring that they pass within 0.2mm (2mm) of the axial beam position for tracks with (without) position measurements in the silicon vertex tracker.

To reconstruct Z^0 candidates, we form all unique combinations of pairs of electrons in the event. To avoid rejecting events where the charge of one electron is misidentified, we do not impose an opposite charge requirement on the pair. We ensure that all electron candidates are isolated from each other by requiring a separation of 0.2 in ΔR between any two electron candidates in the combination. If both candidates in a pair have associated tracks, we ensure they are consistent with originating from the same parent by requiring their z_0 measurements to lie within 5 cm of each other. The invariant mass distributions for events containing Z^0 candidates formed from a "seed" electron candidate together with just one other electron candidate and the subset where an isolated track is used as the second electron candidate are shown in Fig. 1.

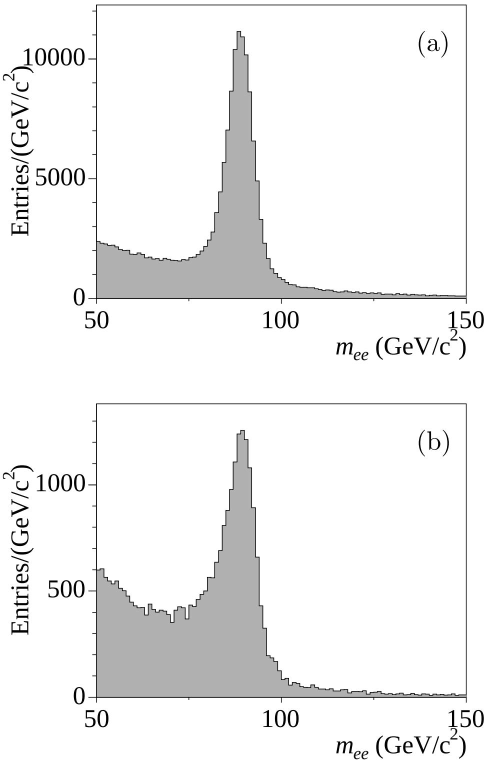

FIG. 1: Distribution of m_{ee} for Z^0 candidates formed from a "seed" electron candidate together with a second electron candidate (a), and the subset of Z^0 candidates formed from a "seed" electron candidate and an isolated track (b).

To reconstruct Z^0 pairs, we form all unique combinations of all Z^0 candidates containing a "seed" electron with all other Z^0 candidates in the event and again require a separation of 0.2 in ΔR between any two electrons in the four-electron combination.

The variable

$$\chi^2 = \sum_{i=1,2} \left(\frac{m_i - m_{Z^0}}{\sigma_i} \right)^2 \qquad (1)$$

quantifies consistency between a given combination and a $Z^0 Z^0 \to eeee$ final state, where $m_{\mathrm{Z}^0} = 91.19$ GeV/c^2 is the nominal Z^0 mass [18], m_i is the measured invariant mass of each candidate Z^0 in the combination computed from the electron candidates' four-momenta, and σ_i is the

TABLE I: Electron Selection Criteria

Criteria	Central (Seed)	Forward	Track
E_{T} (GeV)	$\geq 5(20)$	≥ 5	
$\lvert z_0 \rvert$ (cm)	< 60		< 60
E_{HAD}/E_{EM}	$< 0.055 + 0.00045\,\mathrm{GeV}^{-1} \times E$	< 0.05	
Isolation	< 0.2	< 0.2	> 0.9
p_T (GeV/c)	(≥ 10)		≥ 10

uncertainty on the mass of each Z^0 candidate consisting of a contribution from the intrinsic width of the Z^0 boson and a contribution propagated from the individual electron energy or momentum measurements (typically ~ 3.5 GeV/c^2). In each event, we retain the one Z^0Z^0 combination with the lowest χ^2.

We fix the final event selection criteria before examining the event yield in the signal region. We define the signal region as the events containing a four electron combination with $\chi^2 < 50$ and $m_{eeee} > 500$ GeV/c^2. Events with $m_{eeee} < 400$ GeV/c^2 are used as a low-mass control region to estimate backgrounds, as described in Section IV. We find 12 events containing four electron candidates in this control region.

Although we do not focus on one specific model, for the purpose of quantifying acceptance for this signature, we consider a graviton-production scenario implemented in the HERWIG [20] Monte Carlo generator which is treated in a model-independent way, assuming only that there is a universal coupling of the graviton to standard-model particles. For comparison, we interpret the couplings in the context of the RS1 model. We determine geometric and kinematic acceptance and reconstruction efficiency for this model using Monte Carlo calculations followed by a GEANT-based simulation of the CDF II detector [19]. We consider graviton production followed by decay to two Z^0 bosons followed by decay into four electrons. We use a leading-order calculation implemented in HERWIG to estimate acceptance times efficiency for the model. For a RS1 graviton with mass $M_G = 500$ GeV/c^2 and ratio of warp factor to Planck mass, $k/\overline{M}_{Pl} = 0.1$, Fig. 2 shows the distribution of reconstructed χ^2 and m_{eeee}, the invariant mass of the Z^0Z^0 combination with the lowest χ^2 computed from the four-momenta of the two Z^0 candidates. As expected for events containing two real Z^0 bosons, the χ^2 distribution peaks near zero, and the total invariant mass of selected combinations is centered on the generated graviton mass (500 GeV/c^2). Events which contain mis-measured electrons contribute to the population with large χ^2 values. The width of the m_{eeee} distribution, ~ 15 GeV/c^2, is dominated by the detector resolutions of the constituent electron candidates. We find the geometric and kinematic acceptance times efficiency for this model to be 65%. Of the events recon-

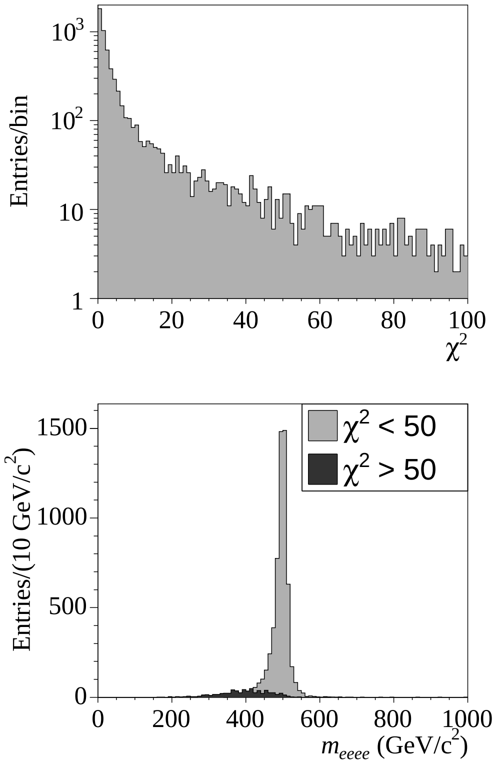

FIG. 2: Distribution of χ^2 for simulated Randall-Sundrum signal scenario ($m_G = 500$ GeV/c^2) (top). Four-electron invariant mass distribution for events satisfying $\chi^2 < 50$ (gray) and for events which fail this requirement (black) (bottom).

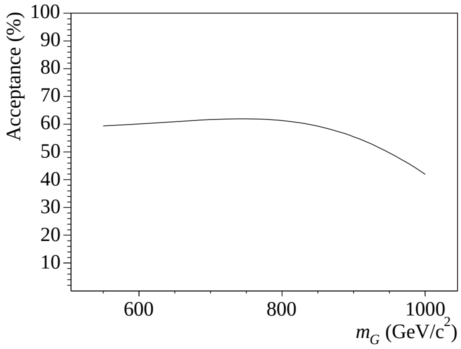

FIG. 3: Acceptance for Randall-Sundrum graviton decaying to Z^0Z^0 versus its mass.

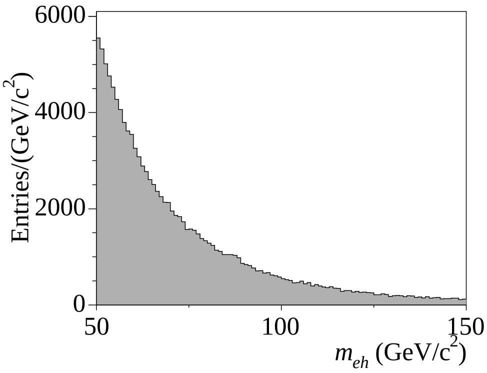

FIG. 4: Invariant mass distribution of one central electron satisfying trigger requirements and one hadronic candidate in data.

structed, 93% yield a four electron combination with $\chi^2 < 50$.

The total acceptance versus m_{eeee} is shown in Fig. 3. At very high graviton mass, the momentum of the daughter Z^0s becomes significant, which can cause the electrons to have a small opening angle and fail the isolation requirement.

IV. BACKGROUND ESTIMATION

In studies using Monte Carlo simulation to estimate the main sources of backgrounds, we find that the dominant background consists of events in which one or more hadrons satisfy the electron ID requirements in the four electron combination.

We use control samples in the data to obtain the shape and normalization of this background in the signal region. Background-dominated (hadron-enriched) control samples are selected from the data. We form hadron candidates, h, from calorimeter clusters in a manner identical to the central and forward electron candidates, with two exceptions. The hadron candidate must fail the relevant E_{HAD}/E_{EM} criterion, and to increase the size of the control samples, we do not impose any isolation requirements. In Fig. 4 we show the invariant mass of all pairings of one seed electron candidate with one hadron candidate. The absence of a significant peak at the Z^0 mass indicates that contamination from electrons in the hadron candidates is small.[1]

We obtain five control samples, namely the four-electron sample which has $m_{eeee} < 400\,\mathrm{GeV}/c^2$ introduced above, and additional control samples having one, two, three, or four hadron candidates by repeating the Z^0Z^0 selection procedure, forming combinations using one or more hadron candidates with electron candidates and retaining the minimum χ^2 combination for each event. The distributions of the minimum χ^2 versus m_{eeee} for samples with different numbers of hadron candidates are shown in Fig. 5. For reconstructed masses smaller than twice the Z^0 mass, there is a correlation between χ^2 and mass caused by a kinematic threshold effect. At higher masses, the two variables are much less correlated.

The single probability density function,

$$f(\chi^2, m_{eeee}) \; = \; Cm_{eeee}^{\gamma}e^{\chi^2\tau}, \qquad (2)$$

where C is a normalization constant, provides an empirical description of the χ^2 vs. m_{eeee} distributions for each of the four hadron-enriched control samples. We obtain the parameters $\gamma = -4.57 \pm 0.06$ and $\tau = -0.00319 \pm 0.00007$ from a two-dimensional unbinned maximum likelihood fit to the low-mass four-electron control region and the hadron-enriched control samples simultaneously, using events with invariant mass above

[1] The presence of a small amount of electron contamination in the hadron candidate sample has a negligible effect on the estimate of the background at high mass, and is included in the systematic uncertainty we assign to the background estimation method.

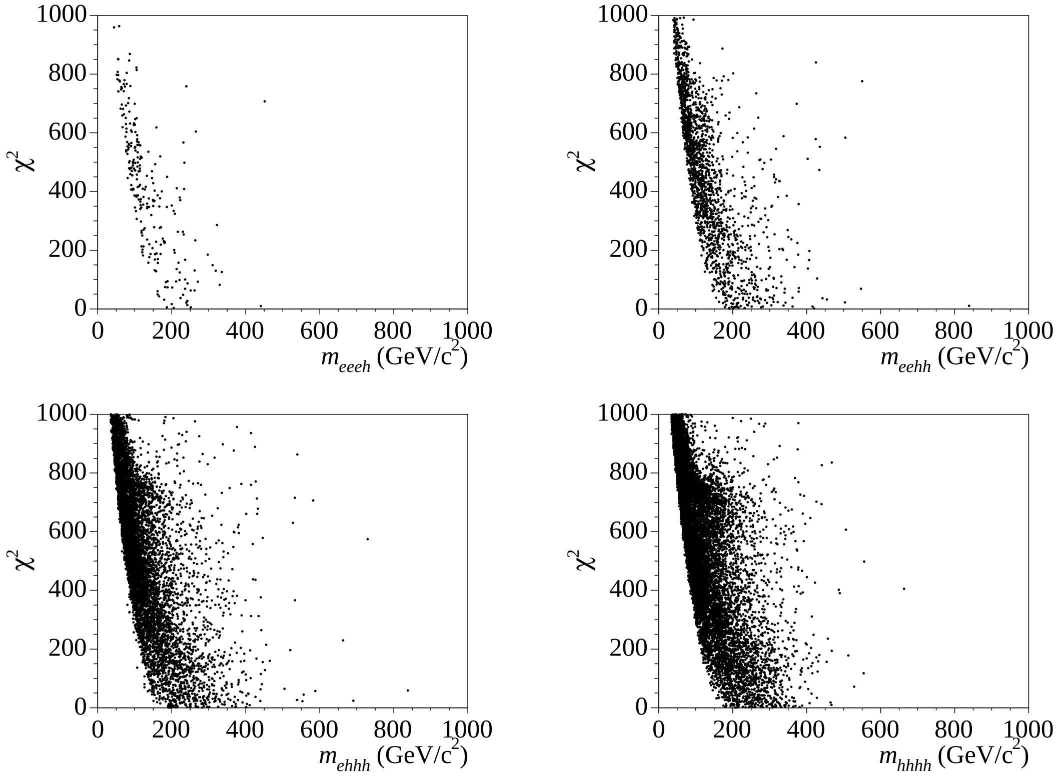

FIG. 5: Distribution of χ^2 vs m_{eeee} for control samples containing one, two, three, or four hadron candidates with the number of events in the plot increasing with the number of hadron candidates used in the combination.

185 GeV/c^2 ($\sim 2 \times m_{Z^0}$.) The control samples containing mostly hadron candidates dominate the fit. Fig. 6 shows the projections of the fit result in the invariant mass dimension along with the data for each hadron-enriched sample. The low-mass control region ($m_{eeee} < 400$ GeV/c^2) contains five events with $m_{eeee} > 185$ GeV/c^2 and serves to normalize the prediction of background in the high-mass search region. We integrate the fit result above 500 GeV/c^2 and $\chi^2 < 50$ to extract an estimate of the total background for the high-mass region. Using this method, we estimate 0.020 ± 0.009 (stat) $\pm$ 0.007 (syst) background events from hadrons misidentified as electrons in the search region. The systematic uncertainty on the background estimate is obtained by varying the functional form of the probability density function fitted to the m_{eeee} spectrum.

We have performed several cross checks to ensure that the fit provides a reasonable estimate of the background rate at high mass. In particular, we have performed the fit allowing the power-law parameter to vary independently for each of the categories. The parameters resulting from this fit along with the number of events observed in each sample are shown in Table II. The fitted values for γ are consistent within errors across categories and with the nominal result. We have verified that the background shape in m_{eeee} is independent of χ^2 in subsets of data in bins of χ^2 and have checked that the projected fit result is consistent with data.

TABLE II: Result of fit with γ floating independently for each control sample.

Sample	Events	γ
eeee	5	-5.90 ± 2.14
eeeh	52	-4.85 ± 0.55
eehh	323	-4.28 ± 0.19
ehhh	1208	-4.43 ± 0.10
hhhh	1927	-4.71 ± 0.09

Standard model production of Z^0Z^0 [21] is the only background to this search with two real Z^0

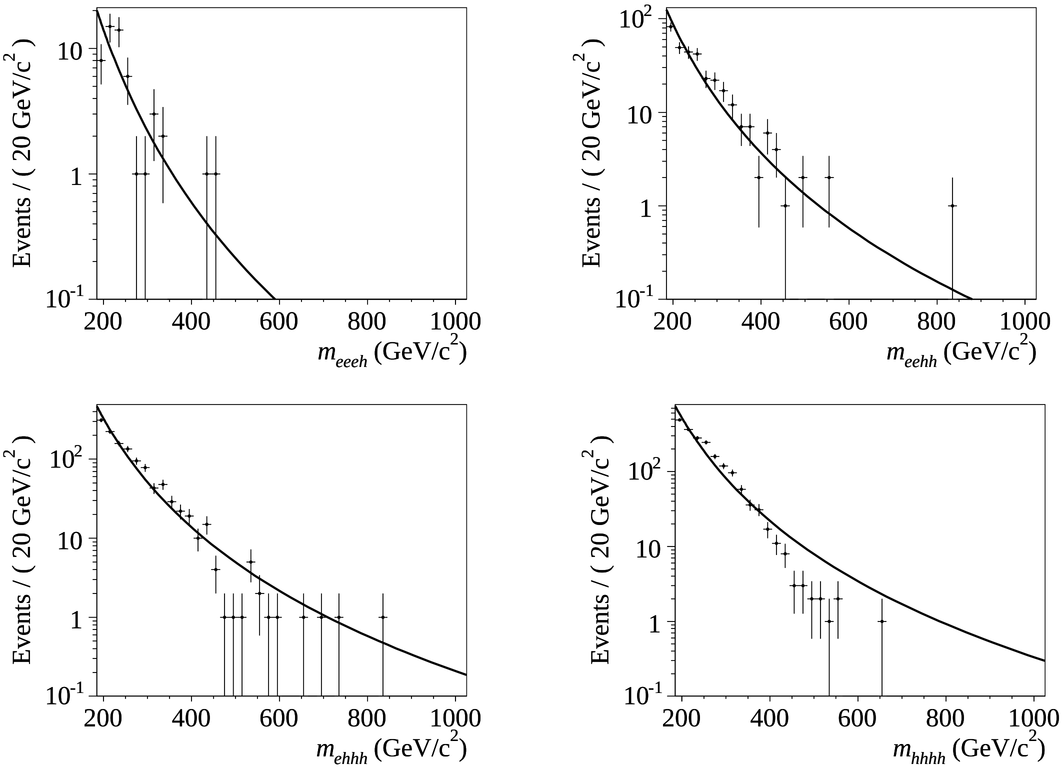

FIG. 6: Projections of fit to invariant mass in control samples of varying number of electron and hadronic candidates with same ordering as in Fig. 5. Data are shown with the fit projection overlaid.

bosons and possibly four electrons in the final state. While we use data to estimate the total background from misidentified electrons in the search region, we have studied the background from this source at high mass with simulated events. We determine geometric and kinematic acceptance using Monte Carlo events generated by PYTHIA [22], followed by a GEANT-based simulation of the CDF II detector. The expected number of events from this background component is determined as the product of the cross section, the luminosity of the sample, and the acceptance of the detector. We estimate a total of 0.54 ± 0.04 events in the four-electron sample. In the invariant mass region above 500 GeV/c^2, we expect 0.008 ± 0.006 events. We estimate the total background from production of standard model Z^0Z^0 events and events in which hadrons are misidentified as electrons is 0.028 ± 0.009 (stat) $\pm$ 0.011 (syst) events.

V. OTHER SYSTEMATIC UNCERTAINTIES

When setting the cross-section limit, we have considered other systematic uncertainties from several sources. The dominant source of these uncertainties is from the measured luminosity (5.9%) [23]. Other sources include parton distribution function uncertainties (0.4%), signal Monte Carlo statistics (1.3%), initial state radiation(1.0%), and the difference between electron identification efficiency in data and simulation (1.0% per electron). The total systematic uncertainty from all these sources is 7.3%.

VI. RESULTS

The distribution of data events surviving all requirements is shown in Fig. 7. We observe no events in the high-mass signal region. There is one event in the low-mass region with very small

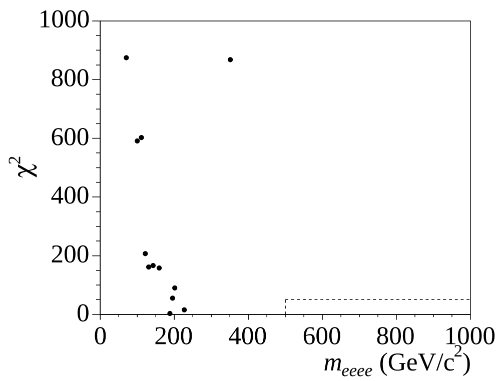

FIG. 7: Distribution of χ^2 vs m_{eeee} for four-electron candidates in data. The signal region is $\chi^2 < 50$ and $m_{eeee} > 500$ GeV/c^2, the boundaries of which are shown by the dashed line.

χ^2 consistent with standard model Z^0Z^0 production, while we expect 0.54 standard model Z^0Z^0 events over the entire mass range. In the observed event, the total invariant mass is 190 GeV/c^2, and the two Z^0 candidates in the lowest χ^2 combination have measured masses of 91 and 92 GeV/c^2.

We have set limits on $\sigma(p\bar{p} \to G) \times \mathrm{BF}(G \to Z^0Z^0)$ in the context of a RS1 graviton scenario. We use a Bayesian binned maximum likelihood method to extract 95% confidence level limits in 100 GeV/c^2 wide windows centered on each mass. We incorporate the effects of uncertainty on the background and signal acceptance with a flat prior for the signal rate and Gaussian priors for the acceptance and expected background. The limits including systematic uncertainties on the acceptance on $\sigma \times \mathrm{BF}(G \to Z^0Z^0)$ range from 4−6 pb, depending on the graviton mass, and are shown in Fig. 8 along with the prediction from the RS1 model for $k/\overline{M}_{Pl} = 0.1$. In the future, the sensitivity of this search will improve with more data as well as additional acceptance from other Z^0 decays.

VII. CONCLUSIONS

We have searched for production of particles decaying to a pair of Z^0 bosons. We have estimated backgrounds from misidentified electrons using a data-based technique, and the background from standard model processes involving four electrons with simulations. Using an optimized electron selection, we expect 0.028 ± 0.009 (stat) ± 0.011 (syst) total background events with $\chi^2 < 50$ above 500 GeV/c^2 in 1.10 fb^{-1}, and observe no events. In the absence of evidence for a signal, we have set limits on $\sigma(p\bar{p} \to G(1.96\,\mathrm{GeV})) \times \mathrm{BF}(G \to Z^0Z^0)$.

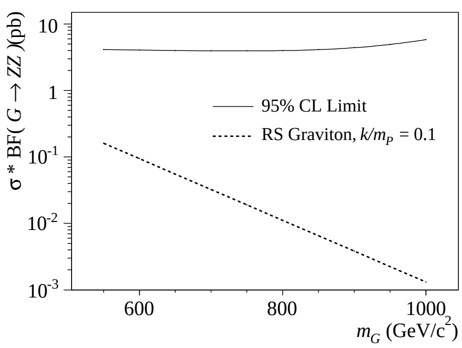

FIG. 8: Limits on $\sigma \times \mathrm{BF}(G \to Z^0Z^0)$ versus mass.

Acknowledgments

We thank the Fermilab staff and the technical staffs of the participating institutions for their vital contributions. This work was supported by the U.S. Department of Energy and National Science Foundation; the Italian Istituto Nazionale di Fisica Nucleare; the Ministry of Education, Culture, Sports, Science and Technology of Japan; the Natural Sciences and Engineering Research Council of Canada; the National Science Council of the Republic of China; the Swiss National Science Foundation; the A.P. Sloan Foundation; the Bundesministerium für Bildung und Forschung, Germany; the Korean Science and Engineering Foundation and the Korean Research Foundation; the Science and Technology Facilities Council and the Royal Society, UK; the Institut National de Physique Nucleaire et Physique des Particules/CNRS; the Russian Foundation for Basic Research; the Comisión Interministerial de Ciencia y Tecnología, Spain; the European Community's Human Potential Programme; the Slovak R&D Agency; and the Academy of Finland.

[1] A. Abulencia *et al.* (CDF Collaboration), Phys. Rev. Lett. **98**, 161801 (2007).
[2] V. M. Abazov *et al.* (D0 Collaboration), Phys. Rev. Lett. **95**, 141802 (2005).
[3] A. A. Affolder *et al.* (CDF Collaboration), Phys. Rev. Lett. **88**, 071806 (2002).
[4] D. E. Acosta *et al.* [CDF Collaboration], Phys. Rev. D **71**, 091105 (2005) [arXiv:hep-ex/0501021].
[5] L. Randall and R. Sundrum, Phys. Rev. Lett. **83**, 3370 (1999).
[6] L. Randall and R. Sundrum, Phys. Rev. Lett. **83**, 4690 (1999).
[7] B. C. Allanach, K. Odagiri, M. J. Palmer, M. A. Parker, A. Sabetfakhri and B. R. Webber, JHEP **0212**, 039 (2002)
[8] T. Aaltonen *et al.* (CDF Collaboration),
[9] T. Aaltonen *et al.* (CDF Collaboration), arXiv:hep-ex/07072524.
[10] V. M. Abazov *et al.* (D0 Collaboration), Phys. Rev. Lett. **95**, 091801 (2005).
[11] A. L. Fitzpatrick, J. Kaplan, L. Randall, and L. T. Wang, J. High Energy Phys. **0709**, 013 (2007).
[12] D. Acosta *et al.* (CDF Collaboration), Phys. Rev. D **71**, 032001 (2005).
[13] A. Sill *et al.*, Nucl. Instrum. Methods A **447**, 1 (2000). A. A. Affolder *et al.*, Nucl. Instrum. Methods A **453**, 84 (2000).
[14] CDF uses a cylindrical coordinate system in which θ (ϕ) is the polar (azimuthal) angle, r is the radius from the nominal beam axis, and $+z$ points along the proton beam direction and is zero at the center of the detector. The pseudorapidity is defined as $\eta \equiv -\ln\tan(\theta/2)$. Energy (momentum) transverse to the beam is defined $E_{\mathrm{T}} \equiv E\sin\theta$ ($p_T \equiv p\sin\theta$), where E is energy measured by the calorimeter and p is momentum measured by the spectrometer.
[15] A. A. Affolder *et al.*, Nucl. Instrum. Methods A **526**, 249 (2004).
[16] L. Balka *et al.*, Nucl. Instrum. Methods A **267**, 272 (1988).
[17] D. Acosta *et al.*, Nucl. Instrum. Methods A**494**, 57 (2002).
[18] W.-M. Yao *et al.*, J. Phys. G **33**, 1 (2006).
[19] R. Brun, F. Bruyant, M. Maire, A. C. McPherson and P. Zanarini, "GEANT3," CERN Report No. CERN-DD/EE/84-1 (unpublished).
[20] G. Corcella *et al.*, "HERWIG 6: An event generator for hadron emission reactions with interfering gluons (including supersymmetric processes)," J. High Energy Phys **0101**, 010 (2001).
[21] J. M. Campbell and R. K. Ellis, Phys. Rev. D **60**, 113006 (1999).
[22] T. Sjostrand, S. Mrenna, and P. Skands, "PYTHIA 6.4 physics and manual," J. High Energy Phys. **0605**, 026 (2006).
[23] S. Klimenko, J. Konigsberg, and T.M. Liss, FERMILAB-FN-0741 (2003) (unpublished).